

THE ENERGY DEPENDENCE OF THE TOTAL CHARM CROSS-SECTION* **

RAMONA VOGT

Lawrence Livermore National Laboratory
Livermore, CA 94551, USA

and

Department of Physics, University of California at Davis
Davis, CA 95616, USA

(Received October 16, 2008)

We discuss the energy dependence of the total charm cross-section and some of its theoretical uncertainties including the quark mass, scale choice and the parton densities. We compare the next-to-leading order calculation of the total cross-section with results obtained using PYTHIA.

PACS numbers: 13.85.Ni, 25.75.Dw

1. Introduction

Extracting the total charm cross-section from data is a non-trivial task. Early fixed-target data were at rather low p_T , making the charm quark mass the most relevant scale. At proton and ion colliders, although the RHIC experiments can access the full p_T range and thus the total cross-section, the data reach rather high p_T , $p_T \gg m$, making p_T (m_T) the most relevant scale. Here we focus on the total cross-section calculation where the quark mass is the only relevant scale.

2. Next-to-leading order pQCD

The hadronic cross-section in pp collisions can be written as

$$\sigma_{pp}(S, m^2) = \sum_{i,j=q,\bar{q},g} \int dx_1 dx_2 f_i^p(x_1, \mu_F^2) f_j^p(x_2, \mu_F^2) \hat{\sigma}_{ij}(s, m^2, \mu_F^2, \mu_R^2), \quad (1)$$

where x_1 and x_2 are the fractional momenta carried by the colliding partons and f_i^p are the proton parton densities. The partonic cross-sections [1]

* Presented at the XXXVII International Symposium on Multiparticle Dynamics, Berkeley, USA, August 4–9, 2007.

** Send any remarks to vogt2@llnl.gov

include $q\bar{q}$ and gg initial states at both $\mathcal{O}(\alpha_s^2)$ and $\mathcal{O}(\alpha_s^3)$ as well as qg and $\bar{q}g$ interactions at $\mathcal{O}(\alpha_s^3)$. At high energies the $q\bar{q}$ and the $\mathcal{O}(\alpha_s^2)$ gg contributions are small while the $\mathcal{O}(\alpha_s^3)$ gg and qg contributions plateau at finite values. Thus, at collider energies, the total cross-sections are primarily dependent on the small x parton densities and phase space.

The perturbative parameters are the charm quark mass and the value of the strong coupling, α_s , while the parton densities are a nonperturbative input. We take $m = 1.5$ GeV as the central value and vary the mass between 1.3 and 1.7 GeV to estimate the mass uncertainties. The perturbative calculation also depends on the unphysical factorization (μ_F) and renormalization (μ_R) scales. The sensitivity of the cross-section to their variation can be used to estimate the perturbative uncertainty due to the absence of higher orders. Since Eq. (1) is independent of the kinematics, we take $\mu_{R,F} = \mu_0 = m$ as the central value and varied the two scales independently within a ‘fiducial’ region defined by $\mu_{R,F} = \xi_{R,F}\mu_0$ with $0.5 \leq \xi_{R,F} \leq 2$ and $0.5 \leq \xi_R/\xi_F \leq 2$. In practice, we use the following seven sets: $\{(\xi_R, \xi_F)\} = \{(1,1), (2,2), (0.5,0.5), (1,0.5), (2,1), (0.5,1), (1,2)\}$. The uncertainties from the mass and scale variations are added in quadrature. The envelope containing the resulting curves defines the uncertainty.

The energy dependence of the total cross-section, calculated with the CTEQ6M parton densities [2], is shown on the left-hand side of Fig. 1. The central value is indicated by the solid curve while the upper and lower edges of the band are given by the dashed curves. The dotted curve on the left-hand side is calculated with $\mu_F = \mu_R = 2m$ and $m = 1.2$ GeV. The uncertainty band broadens as the energy increases. The lower edge of the band grows more slowly with \sqrt{S} above RHIC energies while the upper edge is compatible with the reported total cross-sections at RHIC [3,4].

Next, we discuss the influence of the parton densities on the theoretical uncertainty. Since m is the only perturbative scale, the total cross-section calculations are more sensitive to the low x and low μ behavior of the parton densities. Probing the full fiducial range of the uncertainty band is problematic for charm production since $\xi_F = 0.5$ is below the minimum scale of the CTEQ6M parton densities, $\mu_0^{\text{CTEQ6M}} = 1.3$ GeV [2]. Thus, for this scale, backward evolution is required. The behavior of the gluon density at low scales and low x is atypical, especially for $x < 10^{-2}$. Instead of increasing with decreasing x , for $x < 0.01$, the density decreases and, for $\xi_F = 0.5$, $xg(x)$ can even become zero. This accounts for the high \sqrt{S} behavior of the lower bound on the uncertainty band. The low x , low μ_F behavior of the gluon density depends strongly on how the group performing the global analysis extrapolates to unmeasured regions. All that is required is minimization of the global χ^2 and momentum conservation. The uncertainty band is reduced at higher energies if the GRV98 parton densities [5] are used.

The results are extremely sensitive to the number of flavors, the scale choice and the parton densities, see Ref. [6] for more details. One of the biggest sources of uncertainty at collider energies is the behavior of the gluon density at low x and low scale, as yet not well determined. Until it is further under control, better limits will be difficult to set. A complete NNLO evaluation of the total cross-section may reduce the scale dependence but will still be subject to the same types of uncertainties.

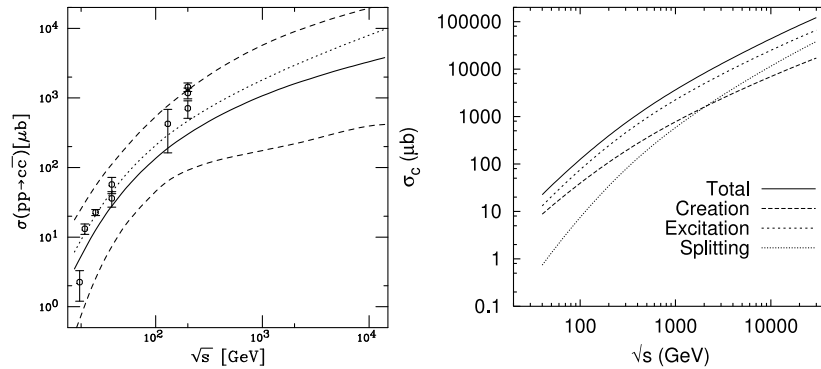


Fig. 1. (Left-hand side) The NLO total charm cross-section uncertainty band in pp interactions calculated with the CTEQ6M PDFs. The central values are given by the solid curves while the dashed curves show the upper and lower limits of the band. The dotted curve on the left-hand side is a calculation with $m = 1.2$ GeV, $\mu_F = \mu_R = 2m$. (Right-hand side) The PYTHIA total charm cross-section in pp interactions. The long-dashed line is the pair creation contribution, the short-dashed line, flavor excitation, and the dotted line, gluon splitting. The sum of the three contributions is given by the solid line [9].

3. PYTHIA calculations

The PYTHIA code [7] has been used extensively to simulate charm production as an alternative to NLO calculations. Since PYTHIA is a leading-order code, to simulate the NLO contributions to heavy flavor production, in addition to the standard leading order pair creation processes, separate calculations of NLO-type processes have to be done. These additional processes are referred to as ‘flavor excitation’ and ‘gluon splitting’ and differ from pair creation by the number of charm quarks in the hard scattering. Pair creation has two charm quarks, flavor excitation has one and gluon splitting has none. Careful separation between the processes is necessary to avoid double counting. However, if done carefully and multiple interactions are turned off while transverse momentum broadening with $\langle k_T^2 \rangle = 1$ GeV²

is implemented, the LO kinematic distributions are essentially identical to those calculated with PYTHIA. Furthermore, the NLO distributions for both $Q\bar{Q}$ pair and single inclusive quantities are very similar to the PYTHIA results with ‘excitation’ and ‘splitting’ included. The only difference in shape appears in the azimuthal angle distributions [8]. The PYTHIA cross-section is somewhat larger than the NLO since it has no interference effects for processes with identical initial states: ‘pair creation’; ‘flavor excitation’ and ‘gluon splitting’ all contribute to the gg channel at NLO. See Ref. [8] for more details.

The right-hand side of Fig. 1 shows the individual contributions to the total charm cross-section obtained using PYTHIA. The energy dependence of the total cross-section is very similar to the NLO dependence. Note that already at rather low energies, the cross-section is not dominated by pair creation but by flavor excitation. At LHC energies, gluon splitting also overtakes pair creation.

This work was performed under the auspices of the US Department of Energy by Lawrence Livermore National Security, LLC, Lawrence Livermore National Laboratory under Contract DE-AC52-07NA27344. The work was also supported in part by the National Science Foundation Grant NSF PHY-0555660. I would also like to thank N. Xu and M. Cacciari for discussions.

REFERENCES

- [1] P. Nason, S. Dawson, R.K. Ellis, *Nucl. Phys.* **B303**, 607 (1988).
- [2] J. Pumplin *et al.*, *J. High Energy Phys.* **0207**, 012 (2002) [[arXiv:hep-ph/0201195](#)]; D. Stump *et al.*, *J. High Energy Phys.* **0310**, 046 (2003) [[arXiv:hep-ph/0303013](#)].
- [3] J. Adams *et al.* [STAR Collaboration], *Phys. Rev. Lett.* **94**, 062301 (2005) [[arXiv:nucl-ex/0407006](#)].
- [4] A. Adare *et al.* [PHENIX Collaboration], *Phys. Rev. Lett.* **97**, 252002 (2006) [[arXiv:hep-ex/0609010](#)]; S.S. Adler *et al.* [PHENIX Collaboration], *Phys. Rev.* **D76**, 092002 (2007) [[arXiv:hep-ex/0609032](#)].
- [5] M. Glück, E. Reya, A. Vogt, *Eur. Phys. J.* **C5**, 461 (1998).
- [6] R. Vogt, *Eur. Phys. J.* **ST155**, 213 (2008) [[arXiv:0709.2531 \[hep-ph\]](#)].
- [7] T. Sjostrand, S. Mrenna, P. Skands, *J. High Energy Phys.* **0605**, 026 (2006) [[arXiv:hep-ph/0603175](#)].
- [8] M. Bedjidian *et al.*, [arXiv:hep-ph/0311048](#).
- [9] E. Norrbin, T. Sjostrand, *Eur. J. Phys.* **C17**, 137 (2000).